3D Wigner model for a quantum free electron laser with a laser wiggler

M.M. Cola[1,2], L. Volpe[1,2], N. Piovella[1,2], A. Schiavi[3], and R. Bonifacio[2,4]

[1] *Dipartimento di Fisica, Università Degli Studi di Milano, via Celoria 16, I-20133 Milano, Italy*
[2] *INFN - sezione di Milano - via Celoria 16, I-20133 Milano, Italy*
[3] *Dipartimento di Energetica, Università di Roma "La Sapienza" and INFN, Via Scarpa 14, I-00161 Roma, Italy*
[4] *Centro Brasileiro de Pesquisas Físicas, Rio de Janeiro -Brasil*

Abstract

A three dimensional, time dependent quantum model for a FEL with a laser wiggler, based on a discrete Wigner function formalism taking into account the longitudinal momentum quantization, is presented. Starting from the exact quantum treatment, a motion equation for the Wigner function coupled to the self-consistent radiation field is derived in the realistic limit in which the normalized electron beam emittance is much larger than Compton wavelength quantum limit. The model describes the three dimensional spatial and temporal evolution of the electron and radiation beams, including diffraction, propagation, laser wiggler, emittance and quantum recoil effects. It can be solved numerically and reduces to the three dimensional Maxwell-Vlasov model in the classical limit. We discuss the experimental requirements for a Quantum X-ray FEL with a laser wiggler, presenting preliminary numerical results and parameters for a possible future experiment.

Key words: SASE, laser wiggler, Wigner function, 3D effects
PACS: 41.60.Cr, 42.50.Fx, 05.30.-d

1. Introduction

Recently it has been shown that an X-ray Free-Electron laser (FEL) in the self amplified spontaneous emission (SASE) mode can operate in a quantum regime (1) in which the coherence of the emitted radiation can be largely increased (2; 3) with respect to the conventional FEL sources (4; 5; 6). The transition from the classical FEL to the Quantum FEL (QFEL) occurs when $\bar{\rho} < 1$, where $\bar{\rho} = \rho(mc\gamma_r/\hbar k_r)$ (1) and ρ is the FEL parameter (7). The QFEL parameter $\bar{\rho}$ is approximately equal to the ratio between the maximum classical momentum spread (of the order of $mc\gamma_r\rho$) and the photon recoil momentum $\hbar k_r$, and yields also the maximum number of photons emitted per electron in a high-gain classical FEL.

A discussion of the main features of QFEL in the SASE mode operation is presented elsewhere in these Proceedings (8). Here we present the three dimensional (3D), time dependent quantum description of a FEL with a laser wiggler, based on the Wigner function for the electron beam (9).

It has been shown that, in order to realize a QFEL, a laser wiggler must be used (10; 11). Such a choice sets some stringent conditions on the electron and laser beam parameters (12), which should be verified by numerical 3D simulations. For this reason, the model of ref.(9) and here presented provides an essential tool to describe a realistic QFEL experiment and determine its parameter constraints.

The following discussion explains why a QFEL requires a laser wiggler instead of a magnetic wiggler (12). The QFEL parameter can be written as $\bar{\rho} = \gamma_r\rho(\lambda_r/\lambda_c)$ where $\lambda_c = h/mc = 0.024$ Å is the Compton wavelength. Using the resonance FEL relation $\gamma_r = \sqrt{\lambda_w(1+a_w^2)/2\lambda_r}$ (where λ_w and a_w are the wiggler period and parameter, respectively), the QFEL condition $\bar{\rho} \leq 1$ yields $\rho \leq \sqrt{2}\lambda_c/\sqrt{\lambda_r\lambda_w(1+a_w^2)}$. Since the high-gain regime needs a wiggler length $L_w \sim \lambda_w/\rho$, then $L_w \geq [\lambda_r\lambda_w^3(1+a_w^2)/2\lambda_c^2]^{1/2}$. If a laser wiggler with a wavelength λ_L is used instead of the magnetic wiggler, then in the above equations $\lambda_w \to \lambda_L/2$. To lase at $\lambda_r \sim 1$Å, a QFEL using a magnetic wiggler with $\lambda_w \sim 1$cm requires a beam energy $E = mc^2\gamma_r \simeq 3.5$ GeV and a wiggler length $L_w \geq 3$Km, whereas using a laser wiggler with $\lambda_L \sim 1\mu$m, $E \simeq 25$MeV and $L_w \geq 2$ mm. Hence, a QFEL using a magnetic wiggler is hard to be conceived, whereas using a laser wiggler it can be a very compact X-ray source.

2. 1D QFEL Wigner model

In a Quantum FEL theory (1; 13), the electrons' system can be described by the Liouville-Von Neumann equation $\partial\hat{\varrho}/\partial\bar{z} = i\left[\hat{H},\hat{\varrho}\right]$ for the electron density operator $\hat{\rho}$, where in the 1D limit the Hamiltonian operator is (14):

$$\hat{H}_{1D}(\bar{z}) = \frac{\hat{p}^2}{2\bar{\rho}^{3/2}} - i\left[A(\bar{z},z_1)e^{i\hat{\theta}} - A^*(\bar{z},z_1)e^{-i\hat{\theta}}\right]. \quad (1)$$

With a circularly polarized counter-propagating laser beam (laser wiggler) instead on the usual magnetic wiggler, the variables and the parameters in Eq.(1) are defined as follows: $\theta = (k_r+k_L)z - c(k_r-k_L)t - \delta\bar{z}$ is the electron phase, where $k_L = 2\pi/\lambda_L$ and $k_r = 2\pi/\lambda_r$ are the laser and radiation wave numbers, respectively; $p = mc(\gamma-\gamma_0)/(\hbar k_r)$ is the longitudinal momentum, in units of the photon recoil momentum, $\hbar k_r$, and $\delta = mc(\gamma_0-\gamma_r)/(\bar{\rho}\hbar k_r)$ is the detuning, where γ_0 and $\gamma_r = [\lambda_L(1+a_0^2)/4\lambda_r]^{1/2}$ are the initial and resonant electron energy in mc^2 units, respectively; the position along the wiggler $\bar{z} = z/L_g$ is expressed in gain length units $L_g = \lambda_L/(8\pi\rho\sqrt{\bar{\rho}})$, and the electron position along the beam is $z_1 = (z - v_r t)/(\beta_r L_c)$, where $v_r = c\beta_r$ is the resonant velocity and $L_c = \lambda_r/(4\pi\rho\sqrt{\bar{\rho}})$ is the cooperation length; $\rho = (1/2\gamma_r)(I/I_A)^{1/3}(\lambda_L a_0/4\pi\sigma)^{2/3}$ is the FEL parameter, I is the beam peak current, $I_A \approx 17kA$ is the Alfvèn current, σ is the transverse rms beam size; $a_0 = eE_0/mc^2k_L$ and E_0 is the laser electric field; A is the slowly varying amplitude of the radiation field, defined such that $|A|^2 = \epsilon_0|E_r|^2/(\hbar\omega_r n_b)$ is the average number of photons emitted per electron in the electron beam volume, E_r is the radiation electric field, $n_b = I/(2\pi\sigma^2 ec)$ is the electron density and $\omega_r = ck_r$. The operators associated to the electron position θ and momentum p are $\hat{\theta}$ and $\hat{p} = -i\partial/\partial\theta$, so that $[\hat{\theta},\hat{p}] = i$. In this formalism $\bar{z}$ takes the role of the "time", whereas z_1 is the longitudinal coordinate in the electron rest frame and appears in Eq.(1) as a parametric dependence in the classical field amplitude A.

The 1D discrete Wigner function representation (15) of the statistic operator $\hat{\varrho}$ is

$$W_n\ (\theta,\bar{z};z_1) = \\ = w_n(\theta,\bar{z};z_1) + \sum_{m\in\mathbb{Z}} \frac{(-1)^{n-m-1}}{(n-m-1)\pi} w_{m+\frac{1}{2}}(\theta,\bar{z};z_1), \quad (2)$$

where

$$w_s\ (\theta,\bar{z};z_1) = \\ = \frac{1}{2\pi}\int_{-\pi}^{+\pi} d\theta' e^{-i2s\theta'} \left\langle \theta+\theta' \right| \hat{\varrho}(\bar{z};z_1) \left| \theta-\theta' \right\rangle \quad (3)$$

and $s = n$ or $s = n+1/2$, with $n \in \mathbb{Z}$. Notice that w_s has indexes both integer and half-integer and w_n and $w_{n+1/2}$ are periodic functions of θ, with a period π and 2π, respectively. With these definitions, it has been shown that a QFEL can be described in the 1D limit by the following equations (16):

$$\frac{\partial w_s}{\partial\bar{z}} + \frac{s}{\bar{\rho}^{3/2}}\frac{\partial w_s}{\partial\theta} - \left(Ae^{i\theta} + A^*e^{-i\theta}\right)\left(w_{s+\frac{1}{2}} - w_{s-\frac{1}{2}}\right) = 0 \quad (4)$$

$$\frac{\partial A}{\partial\bar{z}} + \frac{\partial A}{\partial z_1} = \sum_{m=-\infty}^{+\infty}\int_{-\pi}^{+\pi} \mathrm{d}\theta e^{-i\theta} w_{m+\frac{1}{2}} + i\delta A \quad (5)$$

Notice that the momentum quantization appears in Eq.(4) as a finite-difference in the interaction term with the electromagnetic field.

3. 3D QFEL description

3.1. *Basic considerations*

The one-dimensional analysis of the quantum FEL suggests that an experiment in the X-ray region, confirming the existence of the "quantum purification" phenomenon (2; 3; 8), could be envisaged in a near future. Therefore, the extension of the 1D quantum model to a "more realistic" 3D scheme is more than ever necessary. In a classical framework, the extension from 1D to 3D is rather straightforward, as shown by the different classical models in the literature (17; 18; 19; 20). Several SASE-FEL experiments based on these theory are actually in progress (4; 5; 6) and some numerical, experimental friendly codes were been developed for the 3D simulations, as for instance `GENESIS` (21).

The extension from 1D to a 3D theory in a quantum framework is not so straightforward as in the classical case. This fact is principally linked to the different nature of the electron-radiation interaction along the longitudinal and transverse directions. In fact, whereas along the longitudinal axis the photon recoil effect is dominant and needs a quantum description, instead in the transverse dynamics the quantum effects appear less relevant. For these reasons, a model describing either the quantum behavior along the longitudinal axis *and* the approximately classical behavior along the transverse coordinates, is demanded.

Our intent is to obtain a set of coupled equations which describe the 3D evolution of the electron beam interacting with the laser wiggler field and the self-consistent emitted radiation field. This set of equations should admit three fundamental limits:

(i) transverse classical limit *i.e.* there should exist a parameter ruling the transition from the quantum to the classical behavior for the transverse motion only;
(ii) 1D limit *i.e.* the 3D equations should reduce to Eqs.(4)-(5) when transverse effects are neglected;
(iii) full classical limit *i.e.* the 3D equations should reduce to the 3D classical Maxwell-Vlasov equations when $\bar{\rho} << 1$.

3.2. *3D Wigner model*

In a quantum description, the evolution of the electron density operator $\hat{\rho}$ is determined by the following 3D Hamil-

tonian operator:

$$\hat{H}_{3D}(\bar{z}) = \frac{\hat{p}^2}{2\bar{\rho}^{3/2}} + \frac{\alpha b}{2}\hat{p}_t^2 + \frac{\xi}{\alpha\rho\sqrt{\bar{\rho}}X}|g(\hat{\bar{\mathbf{x}}}_t,\bar{z})|^2$$
$$-i\left[g^*(\hat{\bar{\mathbf{x}}}_t,\bar{z})A(\hat{\bar{\mathbf{x}}}_t,\bar{z},z_1)e^{i\hat{\theta}} - g(\hat{\bar{\mathbf{x}}}_t,\bar{z})A^*(\hat{\bar{\mathbf{x}}}_t,\bar{z},z_1)e^{-i\hat{\theta}}\right]$$
$$+\left[\frac{\xi}{2\rho\sqrt{\bar{\rho}}}\left(1-|g(\hat{\bar{\mathbf{x}}}_t,\bar{z})|^2\right) - \frac{bX}{4}\alpha^2\hat{p}_t^2\right]\hat{p}. \qquad (6)$$

This expression includes the transverse electron dynamics and the field and laser wiggler spatial dependence. The transverse momentum operator $\hat{\mathbf{p}}_t = -i\nabla_{\bar{\mathbf{x}}_t}$ is associated with the variable $\mathbf{p}_t = (\gamma_r\sigma/\lambda\!\!\!^{-}_c)\,\mathbf{x}'_t$ (where $\mathbf{x}'_t = d\mathbf{x}_t/dz$ and $\lambda\!\!\!^{-}_c = \hbar/mc$ is the Compton wavelength), and it is canonically conjugated to the transverse position operator $\hat{\bar{\mathbf{x}}}_t = \hat{\mathbf{x}}_t/\sigma$, with commutation rules $[\hat{\bar{x}}_x,\hat{p}_x] = [\hat{\bar{x}}_y,\hat{p}_y] = i$. The parameters appearing in Eq.(6) are $\alpha = \lambda\!\!\!^{-}_c/\epsilon_n$, where ϵ_n is the normalized beam transverse emittance, $X = 4\pi\epsilon_n/(\gamma_r\lambda_r)$, $\xi = a_0^2/(1+a_0^2)$ and $b = L_g/\beta^*$, where $\beta^* = \sigma^2\gamma_r/\epsilon_n$. In Eq.(6) the second term $(\alpha b/2)\hat{p}_t^2 = -L_g(\lambda\!\!\!^{-}_c/2\gamma_r)\nabla^2_{\mathbf{x}_t}$ is the transverse kinetic energy, the third term describes the change of the FEL resonance due to variation of the laser wiggler profile and to beam angular spread. The transverse laser wiggler amplitude profile is described by $g(\bar{\mathbf{x}}_t,\bar{z})$ (equal to unity in the 1D model). In the 3D description, the Wigner functions (3) are

$$w_s\ (\theta,\bar{\mathbf{x}}_t,\mathbf{p}_t,\bar{z};z_1) = \frac{1}{2\pi^3}\int_{-\pi}^{+\pi}d\theta'\int d^2\bar{\mathbf{x}}'_t\ e^{-2\,i(s\theta'+\bar{\mathbf{x}}'_t\cdot\,\mathbf{p}_t)}$$
$$\cdot\,\langle\theta+\theta',\bar{\mathbf{x}}_t+\bar{\mathbf{x}}'_t|\,\hat{\varrho}(\bar{z};z_1)\,|\,\bar{\mathbf{x}}_t-\bar{\mathbf{x}}'_t,\,\theta-\theta'\rangle\,, \qquad (7)$$

where s is integer or half-integer. Tracing the Wigner function over one variable, we obtain the probability distribution for the other variables. In particular, the momentum distribution is

$$P_m(\mathbf{p}_t,\bar{z};z_1) = \int_{-\pi}^{+\pi}d\theta\int d^2\bar{\mathbf{x}}_t\,w_m(\theta,\bar{\mathbf{x}}_t,\mathbf{p}_t,\bar{z};z_1), \qquad (8)$$

and the position distribution is

$$Q\ \ (\theta,\bar{\mathbf{x}}_t,\bar{z};z_1) = \sum_m\int d^2\mathbf{p}_t$$
$$\cdot\left\{w_m(\theta,\bar{\mathbf{x}}_t,\mathbf{p}_t,\bar{z};z_1) + w_{m+\frac{1}{2}}(\theta,\bar{\mathbf{x}}_t,\mathbf{p}_t,\bar{z};z_1)\right\}. \qquad (9)$$

Note that the half-integer functions $w_{m+1/2}$ do not contribute to the integral in P_m (15). As a consequence

$$\sum_m\int_{-\pi}^{+\pi}d\theta\int d^2\mathbf{p}_t\,w_m(\theta,\bar{\mathbf{x}}_t,\mathbf{p}_t,\bar{z};z_1) = J(\bar{\mathbf{x}}_t,\bar{z};z_1) \qquad (10)$$

is the current density (normalized to unity at the peak) and

$$\int d^2\bar{\mathbf{x}}_t J(\bar{\mathbf{x}}_t,\bar{z};z_1) = I_0(z_1) \qquad (11)$$

is the stationary longitudinal beam profile (3).

Differentiating Eq.(7) and inserting in it the Liouville-Von Neumann equation for $\hat{\varrho}$ with the Hamiltonian operator of Eq.(6), a long but not trivial calculation allows to obtain an integro-differential evolution equation for the Wigner function w_s. This equation describes an electron beam with a transverse normalized emittance till to the 'ultracold' limit of the Compton wavelength, $\epsilon_n \simeq \lambda\!\!\!^{-}_c$. In fact, the transverse momentum distribution is bounded below by the Heisenberg's Uncertainty Principle only, $\Delta x\Delta p_x \geq \hbar$. Using $\Delta p_x = mc\gamma_r\Delta x'$ and $\epsilon_n = \gamma_r\Delta x\Delta x'$, we obtain $\varepsilon_n \geq \lambda\!\!\!^{-}_c$. However, we are interested in describing only electron beams in which the transverse momentum distribution is thermal, with a width $\Delta x' \sim \epsilon_n/(\sigma\gamma_r)$ much larger than the quantum limit $\lambda\!\!\!^{-}_c/(\sigma\gamma_r)$. Such a state will be necessary a mixed state with $\Delta x\Delta p_x \gg \hbar$ and this allows to perform some simplifications to the equation for the Wigner function. To this propose, we introduce $\alpha = \lambda\!\!\!^{-}_c/\epsilon_n$, given by the ratio between the "quantum limit emittance" and the normalized emittance.

Since with the present technology $\alpha \ll 1$, we can write our model equations as a α-power expansion and retain only lower terms. In particular, keeping only the zero-order term (corresponding to zero-order in $\hbar$) the following equations are obtained:

$$\frac{\partial w_s}{\partial\bar{z}} + b\,\bar{\mathbf{p}}_t\cdot\nabla_{\bar{\mathbf{x}}_t}w_s - \left(g^*Ae^{i\theta} - gA^*e^{-i\theta}\right)\left[w_{s+\frac{1}{2}} - w_{s-\frac{1}{2}}\right]$$
$$+\left\{\frac{s}{\bar{\rho}^{3/2}} + \frac{\xi}{2\rho\sqrt{\bar{\rho}}}(1-|g|^2) - \frac{b^2}{4a}\bar{p}_t^2\right\}\frac{\partial w_s}{\partial\theta}$$
$$-\frac{\xi}{\rho\sqrt{\bar{\rho}}X}\nabla_{\bar{\mathbf{x}}_t}|g|^2\cdot\nabla_{\bar{\mathbf{p}}_t}w_s = 0 \qquad (12)$$

$$\frac{\partial A}{\partial\bar{z}} + \frac{\partial A}{\partial z_1} - ia\nabla^2_{\bar{\mathbf{x}}_t}A - i\delta A$$
$$= g\sum_m\int d^2\bar{\mathbf{p}}_t\int_{-\pi}^{+\pi}d\theta e^{-i\theta}w_{m+\frac{1}{2}}, \qquad (13)$$

where $a = L_g/Z_r = b/X$ is the diffraction parameter and $Z_r = 4\pi\sigma^2/\lambda$ is the Rayleigh range of the emitted radiation with a transverse radius equal to the electron beam radius.

It is important to note that Eq.(12) reduces to a Vlasov equation in the classical limit $\bar{\rho} \gg 1$. In fact, switching to the classical FEL scaling (*i.e.* $A = \sqrt{\bar{\rho}}A_c$, $\bar{z} = \sqrt{\bar{\rho}}\bar{z}_c$, $z_1 = \sqrt{\bar{\rho}}z_{1c}$, $\delta = \delta_c/\sqrt{\bar{\rho}}$, $b = b_c/\sqrt{\bar{\rho}}$ and $a = a_c/\sqrt{\bar{\rho}}$, see (14)), for $\bar{\rho}\to\infty$ the new longitudinal momentum, $\bar{p} = s/\bar{\rho}$, can be treated as a continuous variable and

$$w_s(\theta,\bar{\mathbf{x}}_t,\bar{\mathbf{p}}_t,\bar{z};z_1) \to \bar{\rho}f(\theta,\bar{p},\bar{\mathbf{x}}_t,\bar{\mathbf{p}}_t,\bar{z}_c;z_{1c}) \qquad (14)$$
$$\left[w_{s+\frac{1}{2}}(\theta,...) - w_{s-\frac{1}{2}}(\theta,...)\right] \to \qquad (15)$$
$$\to\bar{\rho}\left[f(\theta,\bar{p}+\frac{1}{2\bar{\rho}},...) - f(\theta,\bar{p}-\frac{1}{2\bar{\rho}},...)\right] \to \frac{\partial}{\partial\bar{p}}f\,(\theta,\bar{p},...)$$

where f is a classical electron distribution function. In this limit, Eqs. (12) and (13) reduce to the classical Vlasov-Maxwell equations:

$$\frac{\partial f}{\partial \bar{z}_c} + b_c \bar{\mathbf{p}}_t \cdot \nabla_{\bar{\mathbf{x}}_t} f + \left\{ \bar{p} + \frac{\xi}{2\rho}(1-|g|^2) - \frac{b_c^2}{4a_c}\bar{p}_t^2 \right\} \frac{\partial f}{\partial \theta}$$
$$- \left(g^* A_c e^{i\theta} + g A_c^* e^{-i\theta} \right) \frac{\partial f}{\partial \bar{p}} - \frac{\xi}{\rho X} \nabla_{\bar{\mathbf{x}}_t} |g|^2 \cdot \nabla_{\bar{\mathbf{p}}_t} f = 0 \quad (16)$$

$$\frac{\partial A_c}{\partial \bar{z}_c} + \frac{\partial A_c}{\partial z_{1c}} - i a_c \nabla^2_{\bar{\mathbf{x}}_t} A_c - i \delta_c A_c$$
$$= g \int_{-\pi}^{+\pi} d\theta \int d\bar{p} \int d^2 \bar{\mathbf{p}}_t e^{-i\theta} f. \quad (17)$$

The quantum evolution for w_s, Eq.(12), contains the quantization of the longitudinal momentum in units of $\hbar k_r$ (as the 1D model) and describes the transverse dynamics by the same classical terms appearing in the Vlasov Eq.(16). For the second term in Eq.(12) the following correspondence to unscaled variables holds

$$b\, \bar{\mathbf{p}}_t \cdot \nabla_{\bar{\mathbf{x}}_t} \rightarrow \mathbf{x'}_t \cdot \nabla_{\mathbf{x}_t}. \quad (18)$$

This term describes the transverse drift of the beam, responsible of the beam section increasing from the waist position $\bar{z}_0$ as $\sigma(z) = \sigma\sqrt{1+[(z-z_0)/\beta^*]^2}$ in the free space and for a gaussian beam. The second and third terms in the curl parenthesis in Eq.(12) account for the change of the FEL resonance induced by the laser wiggler profile and by the beam emittance. In particular

$$\frac{b^2}{4a}\bar{p}_t^2 \sim \frac{1}{2\rho\sqrt{\bar{\rho}}} \frac{\epsilon_n^2}{\sigma^2(1+a_0^2)}, \quad (19)$$

where the maximum divergence angle $|\mathbf{x'}_t| \sim \epsilon_n/\gamma_r\sigma$ has been assumed. For the last term in Eq.(12) the following correspondence to unscaled variables holds

$$-\frac{\xi}{\rho\sqrt{\bar{\rho}}X} \nabla_{\bar{\mathbf{x}}_t} |g|^2 \cdot \nabla_{\bar{\mathbf{p}}_t} \rightarrow \mathbf{x''}_t \cdot \nabla_{\mathbf{x'}_t}, \quad (20)$$

where $\mathbf{x''}_t = -(a_0^2/2\gamma_r^2)(\nabla_{\mathbf{x}_t}|g|^2)$ is the ponderomotive force due to the laser transverse gradient.

4. Analysis

A numerical code `QFEL3D` has been developed for solving the coupled Eqs.(12) and (13) based on a Fourier decomposition of the Wigner function and on finite-difference integration of the motion equations on a Cartesian three-dimensional spatial grid (22). In the simulations the initial electron beam was described by a thermal state of energy $mc^2\gamma_0$ and transverse phase space distribution $w_0(\theta, \bar{\mathbf{x}}_t, \bar{\mathbf{p}}_t, 0; z_1) \propto \exp\{-|\bar{\mathbf{x}}_t + b\bar{z}_0\bar{\mathbf{p}}_t|^2/2 - |\bar{\mathbf{p}}_t|^2/2\}$, with the waist position at $\bar{z} = \bar{z}_0$. For simplicity, we did not include in the model the electrons' energy spread, which however can be taken into account by an inhomogeneous broadening in the equation for A, as it has been described in ref. (23).

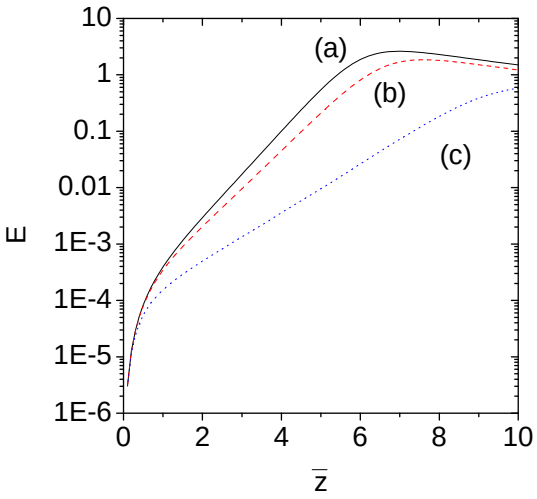

Fig. 1. Total radiated energy, $E(\bar{z}) = \int d^2\bar{\mathbf{x}}_t |A|^2$, vs. $\bar{z}$ for $\bar{\rho} = 0.2$, $a = 1.6 \times 10^{-4}$, $g = 1$ and (a) $b = 0$, (b) $b = \sqrt{a}$, (c) $b = 2\sqrt{a}$. The electron beam focuses at $\bar{z}_0 = 5$.

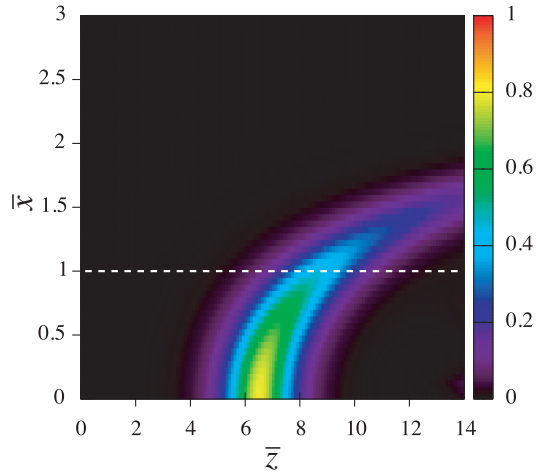

Fig. 2. (Color) Radiation intensity $|A|^2$ as a function of transverse coordinate $\bar{x}$ and of wiggler position $\bar{z}$. Parameters same as for curve (b) in Fig. 1. The dashed line corresponds to the electron beam rms radius σ. As a reference, the 1D model intensity would saturate to unity.

4.1. *Beam requirements for QFEL*

In order to operate a FEL in the high-gain quantum regime, the energy spread must be less than the QFEL line width, *i.e.* $\delta\gamma/\gamma < \rho\sqrt{\bar{\rho}}$. Emittance is an other cause of nonhomogeneous broadening of the radiation line width, due to the beam divergence. In fact, since the resonant wavelength depends on the divergence angle ϑ according to

$$\lambda_r = \frac{\lambda_L(1+a_0^2+\gamma^2\vartheta^2)}{4\gamma^2}, \qquad \text{with} \quad 0 \le \vartheta \le \frac{\epsilon_n}{\gamma\sigma}, \quad (21)$$

we have

$$\frac{\delta\lambda}{\lambda_r} \approx \frac{2\delta\gamma}{\gamma} \approx \frac{\epsilon_n^2}{\sigma^2(1+a_0^2)} \le 2\rho\sqrt{\bar{\rho}}. \quad (22)$$

This inequality can be written, using the definitions of L_g and Z_r, as

$$\epsilon_n \leq \frac{\gamma \lambda_r}{2\pi} \sqrt{\frac{Z_r}{L_g}} \tag{23}$$

or, in terms of our 3D parameters a and b, as

$$\frac{b}{2\sqrt{a}} < 1. \tag{24}$$

This condition arises naturally in our model, since the term (19) in Eq.(12) accounts for the change of the FEL resonance induced by emittance.

An other important constraint on the beam emittance arises when a $\mathtt{TEM}_{00}$ Gaussian laser wiggler is used. In this case

$$g(\bar{\mathbf{x}}_t, \bar{z}) = \frac{1}{[1 - id(\bar{z} - \bar{z}_0)]} \exp\left\{ \frac{-|\bar{\mathbf{x}}_t|^2}{4\sigma_L^2 [1 - id(\bar{z} - \bar{z}_0)]} \right\}, \tag{25}$$

where $\sigma_L = R/\sigma$, $d = L_g/Z_L$, $Z_L = 4\pi R^2/\lambda_L$, and R is the minimum rms laser radius at the beam waist position $\bar{z}_0$. Imposing that the electron beam does not diverge appreciably during the interaction with the laser wiggler, *i.e.* in a laser Rayleigh range Z_L, then

$$\beta^* \geq Z_L \tag{26}$$

or, using the definitions of β^* and Z_L,

$$\epsilon_n \leq \frac{\gamma_r \lambda_L}{4\pi} \left(\frac{\sigma}{R}\right)^2. \tag{27}$$

This condition can be quite restrictive if $\sigma << R$. In terms our dimensionless parameters, Eq.(26) becomes $b \leq d$.

4.2. *Numerical analysis*

Preliminary numerical results have been obtained (9) for the quantum regime, $\bar{\rho} = 0.2$, in steady-state operation mode, i.e. neglecting z_1 dependence. Furthermore, an uniform laser wiggler ($g = 1$) has been assumed, which can be realized for instance using a laser with flattened transverse profile. Such lasers can be produced by suitable transparency films (24) or by overlapping different gaussian beams (25). In both cases, it is possible to realize a laser which remains almost transversally flat within few Rayleigh ranges Z_L from the beam waist.

Assuming $g = 1$, the system depends on the diffraction and emittance parameters only, namely a and b. The interaction is taken over 10 gain lengths ($\bar{z}_{max} = c\tau_{int}/L_g = 10$), with the beam waist in the middle, $\bar{z}_0 = 5$. A set of possible experimental parameters corresponding to this simulation is: $\lambda_r = 2$ Å, $\lambda_L = 1\mu$m, $\gamma_r = 36$, $I = 884$A, $\sigma = 11.5\mu$m and $a_0 = 0.15$ (which could be realized for instance by a laser wiggler with power $P_L \sim 1$TW, duration $\tau_L = 2\tau_{int} = 88$ps and Rayleigh range $Z_L = 6.7$mm). The gain length is $L_g = 1.3$mm, so that the diffraction parameter is $a = 1.6 \times 10^{-4}$. We have considered three different values of the beam emittance in order to investigate its effect on the gain: (a) $\epsilon_n = 0$, i.e. $b = 0$; (b) $\epsilon_n = 0.05$mm-mrad, i.e. $b = \sqrt{a} = 0.013$; (c) $\epsilon_n = 0.1$mm-mrad, i.e. $b = 0.025 = 2\sqrt{a}$. Figure 1 shows the total FEL radiation energy, $E(\bar{z}) = \int d^2\bar{\mathbf{x}}_t |A|^2$, vs. $\bar{z}$ for the cases (a)-(c). Figure 2 shows a color map of the intensity in the plane $(\bar{x}, \bar{z})$ for the (b) case. It can be seen that intensity saturates to a lower level in the beam halo with respect to the beam axis, and that the gain changes along the transverse direction. Notice that the total emitted energy and the on-axis peak intensity can reach a significant fraction of the 1D model for the proposed parameters (b).

5. Conclusions

In summary, we have presented the 3D time dependent quantum model for an FEL with a laser wiggler, which takes into account transverse emittance and radiation diffraction effects, longitudinal propagation effects, the spatial profile of the laser wiggler field as well as the quantum recoil effect along the longitudinal axis. The electron motion is described by a 7D Wigner function, which is continuous in the transverse phase-space and discrete in the longitudinal phase-space variables. Preliminary numerical results have shown that the detrimental effect of the emittance on the gain does not prevent for an exponential amplification of the radiation with reasonable experimental parameters, rather out of the present state of technology, but hopefully available in a near future.

References

[1] R. Bonifacio, M.M. Cola, N. Piovella, and G.R.M. Robb, Europhys. Lett. 69, 55 (2005) .

[2] R. Bonifacio, N. Piovella, G.R.M. Robb, Nucl. Instrum. and Meth. in Phys. Res. A 543, 645 (2005).

[3] R. Bonifacio, N. Piovella, G.R.M. Robb, and A. Schiavi, Phys. Rev. ST Accel. Beams 9, 090701 (2006).

[4] R. Brinkmann et al., TESLA XFEL: First stage of theLCLS Design Study Report, SLAC-R521, Stanford (1998) and http://www-ssrl.slac.stanford.edu/lcls/CDR.

[5] The LCLS Design Study Group: LCLS Design Study Report, SLAC-R521, Stanford (1998) and http://www-ssrl.slac.stanford.edu/lcls/CDR.

[6] T. Shintake, Status of the SCSS Test Accelerator and XFEL Project in Japan', EPAC'06, Edinburgh (2006) and http://www-xfel.spring8.or.jp.

[7] R. Bonifacio, C. Pellegrini and L. Narducci, Opt. Commun. 50, 373 (1984).

[8] R. Bonifacio, N. Piovella, M.M. Cola, L. Volpe, A. Schiavi, and G.R.M. Robb, in these Proceedings.

[9] N. Piovella, M.M. Cola, L. Volpe, A. Schiavi, and R. Bonifacio, *submitted*.

[10] R. Bonifacio, Nucl. Instrum. and Meth. in Phys. Res. A 546, 634 (2005).

[11] R. Bonifacio, M. Ferrario, G.R.M. Robb, N. Piovella, A. Schiavi, L. Serafini, Proceedings of the 27th International Free Electron Laser Conference, 71 (2005).
[12] R. Bonifacio, N. Piovella, M.M. Cola, and L. Volpe, Nucl. Instrum. and Meth. in Phys. Res. A577 (2007) 745.
[13] G. Preparata, Phys. Rev. A 38, 233 (1988).
[14] Here we adopt the quantum FEL scaling (see ref.(1)) instead of the usual classical scaling of ref.(7). In the quantum scaling, $\bar{\rho}$ does not appear explicitely in the solution of the quantum regime, but it is contained in the definition of the variables.
[15] J.P. Bizarro, Phys. Rev. A 49, 3255 (1984).
[16] R. Bonifacio, M.M. Cola, R. Gaiba, L. Volpe, N. Piovella, and A. Schiavi, Opt. Commun. 274, 347 (2007).
[17] N.M. Kroll, P.L. Morton, and M.N. Rosenbluth, IEEE Journ. Quantum Electronics QE-17, 1436 (1981).
[18] T.M. Tran, and J.S. Wurtele, Physics Report 195, 1 (1990).
[19] Y.H. Chin, K.J. Kim and M. Xie *Phys. Rev.A* 46, 6662 (1992).
[20] R. Bacci, M.Ferrario, C.Maroli,V. Petrillo and L. Serafini *Phys. Rev. ST Accel. Beams* 9, 060704 (2006)
[21] S. Reiche, http://pbpl.physics.ucla.edu/ reiche/.
[22] A. Schiavi, M.M. Cola, L. Volpe, N. Piovella, and R. Bonifacio, in these Proceedings.
[23] N. Piovella and R. Bonifacio, Nucl. Instrum. Meth. A 560, 240 (2006).
[24] F. Gori, Opt. Commun. 107, 335 (1994); V. Bagini et al., J. Opt. Soc. Am. A 13, 1385 (1996).
[25] A.A. Tovar, J. Opt. Soc. Am. A 18, 1897 (2001).